High capacity transmission with few-mode fibers

Citation for the original published paper (version of record):
Rademacher, G., Luis, R., Puttnam, B. et al (2019)
High capacity transmission with few-mode fibers
Journal of Lightwave Technology, 37(2): 425-432
http://dx.doi.org/10.1109/JLT.2018.2870038

High Capacity Transmission with Few-Mode Fibers

Georg Rademacher, Ruben S. Luís, Benjamin J. Puttnam, Tobias A. Eriksson, Roland Ryf, Erik Agrell, Ryo Maruyama, Kazuhiko Aikawa, Yoshinari Awaji, Hideaki Furukawa, and Naoya Wada

***Abstract*—We experimentally investigate high-capacity few-mode fiber transmission for short and medium-haul optical links. In separate experiments, we demonstrate C + L band transmission of 283 Tbit/s over a single 30 km span and 159 Tbit/s over 1045 km looped transmission in a graded-index three mode fiber. The first experiment reached a data-rate per fiber mode within 90% of the record data-rates reported in the same transmission bands for single-mode fiber. The second experiment demonstrated the feasibility of reaching high data-rates over long distance few-mode fiber transmission, despite strong impairments due to mode-dependent loss and differential mode delay.**

***Index Terms*—Space Division Multiplexing (SDM), Few-Mode Fiber, High Capacity Transmission**

I. Introduction

SPACE DIVISION MULTIPLEXING (SDM) has gained considerable interest over the last years as a technology to increase the per-fiber data-rates over current single-mode fiber (SMF) technology [1], [2]. In SDM transmission systems, fibers with parallel propagation paths may be used to transmit independent data-streams at the same spectral bands. Suitable fibers for SDM can be either uncoupled multi-core fibers (MCF) [3], where several single-mode fiber cores are arranged inside one fiber cladding or few- and multi-mode fibers (FMF or MMF) [4] where a single fiber core can support the transmission of several orthogonal fiber modes. Hybrid combinations of the two approaches are also attractive and have been used to demonstrate the highest recorded data-rate in a single fiber to date [5], almost 100 times higher than the record throughput in standard SMFs.

While uncoupled single-mode MCFs have certain advantages, such as a potentially easy migration path from current single-mode fiber systems and low receiver complexity, their number of spatial paths is limited by the maximum achievable cladding diameters and inter-core crosstalk. FMFs, however, can support many spatial paths even in a fiber with conventional cladding diameter of 125 μm at the cost of additional digital signal processing (DSP) to undo coupling between different modes that inevitable appears after several km of transmission. Such DSP techniques, generally referred to multi-input / multiple-output (MIMO) processing, rely on low mode-dependent loss (MDL) [6] and reasonably short impulse responses of the transmission system. The length of the impulse response is mostly determined by the fiber design that defines the propagation delay between different modes (differential mode delay, DMD). DMD management, where fibers with negative relative DMD are used to reduce the total delay spread, have also been investigated as a means to minimize the equalizer complexity [7], [8]. To successfully implement a FMF transmission system it is essential to address these issues.

In this paper, we extend two works presented at the optical fiber communication conference (OFC) 2018 [9], [10]. For those experiments, we used a single comb source with a carrier spacing of 25 GHz to generate more than 380 wavelength division multiplexed (WDM) signals across the C and L bands that were transmitted over a three-mode graded-index few-mode fiber. The goal was to achieve per-fiber-mode data-rates comparable to the transmission records in the same bands with single-mode fibers. In addition to the results that were reported in [9], [10], this paper contains a broader background on recent high-capacity SDM transmission demonstrations as well as more detailed information on the observed transmission impairments and on the forward error-correction (FEC) coding scheme that was implemented in [10]. We further applied the same coding scheme on the data for the experiment reported in [9], where we previously assumed a fixed soft-decision FEC threshold for throughput assessment.

II. Recent High Capacity Transmission Achievements with Single-Mode and SDM Fibers

To demonstrate a clear advantage of SDM fibers over SMFs, in addition to multiplying the number of spatial channels it is also important for SDM systems to provide comparable throughput per spatial channel as can be achieved in SMF. Furthermore, such high-capacity transmission should be demonstrated over similar distances and not limited to short transmission reaches of several km. Figure 1 shows the data-rate per spatial channel and the achieved distance for several record SDM demonstrations of the past years as well as SMF transmission systems for reference. The red-dotted lines represent a constant product of data-rate and distance, being a widely used performance metric for optical transmission systems.

Single-mode MCF and SMF have so far dominated the high data-rate per spatial channel-distance-product experiments, while FMF-based transmission experiments were limited to both, relatively short reaches and data-rates. The two experiments that we report in this paper cover two distance regimes: the first one is for short distance with very high data-rates, the second for medium-haul distance of about 1000 km with

Georg Rademacher, Ruben S. Luís, Benjamin J. Puttnam, Tobias A. Eriksson, Hideaki Furukawa, Yoshinari Awaji and Naoya Wada are with the National Institute of Information and Communications Technology, 4-2-1, Nukui-Kitamachi, Koganei, Tokyo, 184-8795, Japan. Roland Ryf is with Nokia Bell Labs, 791 Holmdel Rd., Holmdel, NJ, 07733, USA. Erik Agrell is with Dept. of Electrical Engineering, Chalmers University of Technology, SE-412 96 Gothenburg, Sweden. Ryo Maruyama and Kazuhiko Aikawa are with Fujikura Ltd, 1440, Mutsuzaki, Sakura, Chiba, 285-8550, Japan. (e-mail: georg.rademacher@nict.go.jp).

Manuscript received xxxxx xx, xxxx; revised xxxxxxxx xx, xxxx.

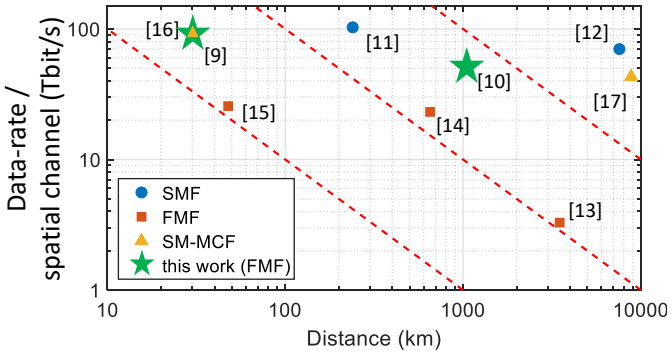

Fig. 1: Recent high capacity transmission demonstrations with single-mode, multi-core and few-mode fibers [9], [10], [11], [12], [13], [14], [15], [16], [17]. Red dashed lines indicate constant data-rate per spatial channel - distance - product.

slightly reduced data-rate. The first experiment constitutes the highest data-rate per spatial channel achieved in an FMF while the second is a record data-rate per spatial channel-distance-product in an FMF. However, we note that Figure 1 also shows that there is still a substantial gap between FMF-based transmission and SMF or single-mode MCF that needs to be closed to fully demonstrate the advantage of FMF technology.

III. FEC Coding Scheme for System Performance Assessment

In the past, it has been common in many transmission demonstrations to assume soft-decision FEC for error free data transmission by including a fixed percentage coding overhead. Typically, a pre-FEC bit error rate (BER) of around 2.7×10^{-2}, corresponding to a Q-factor of 5.7 dB, was assumed to have 20% FEC overhead [18]. However, recent studies have shown that this practice may lead to inaccurate estimations of the required overhead [19]. For the experiments presented in this paper, we chose to calculate the generalized mutual information (GMI) [19], giving the maximum achievable data-rate using a binary soft-decision FEC code and a receiver applying bit-wise decoding and optimal codes with perfectly variable rates per channel. This determines an upper limit of the data-rate for a receiver under certain assumptions described below.

The GMI is calculated assuming code interleaving of all modes per wavelength channel. We model the channel as memoryless additive white Gaussian noise (AWGN) with one noise variance estimated for all modes and assume mismatched decoding. We note that in some cases, higher performance can be achieved by applying more sophisticated channel models in the receiver [20]. However, since most practical decoders, including the ones implemented here, assume an AWGN channel, we make the same assumption in our calculations, too. We also note that in principle, higher data-rates could be achieved by optimizing the rate per mode and polarization. However, this would require several rate-adaptive encoders and decoders per wavelength that might be difficult to implement in practice.

To estimate the performance under more realistic scenarios, we also implement encoding and decoding using low-density parity-check (LDPC) codes from the DVB-2S standard [21] with block length of 64,800 bits and with a finite number of coding rates. We choose six different rates, namely 9/10, 8/9, 5/6, 4/5, 3/4 and 2/3. Loading new patterns in the transmitter adds several inconveniences to the experiments, including a significantly increased measurement time which is unfeasible when measuring a large number of channels as in this experiment. As a result, we apply a Monte Carlo approach for the coding scheme where we generate random binary patterns offline, encode them with the selected code rate, and perform bit-to-symbol mapping. We then emulate the channel by randomly drawing observed noisy samples corresponding to the input symbols of the encoded channel. Note that this approach assumes that a sufficiently large interleaver is used such that any memory effects of the channel are scrambled. We then perform demapping and decoding with up to 40 iterations. Due to the limited number of symbols in the experiments, we cannot feasibly guarantee post-FEC BERs in the order of 10^{-10} or below, as typically used as a required threshold for system operation. To overcome this issue, we assume that an outer hard-decision code is used with 6.25 % overhead [22]. This code can bring the BER of our system below error free BER limits for any output BER of the LDPC decoder that is less than 4.7×10^{-3}. For the throughput calculations, we choose the highest LDPC code rate that gives us a BER below the threshold of the outer FEC. The total throughput is calculated including both the inner and the outer code rate.

The coding scheme assumes a large interleaver between the FEC encoders (and decoders), since the performance of the outer staircase code [22] assumes independent bit errors, while the LDPC decoder produces error bursts. A common type of interleaver is the “row–column interleaver”, which is a matrix buffer where every row corresponds to a codeword of the outer

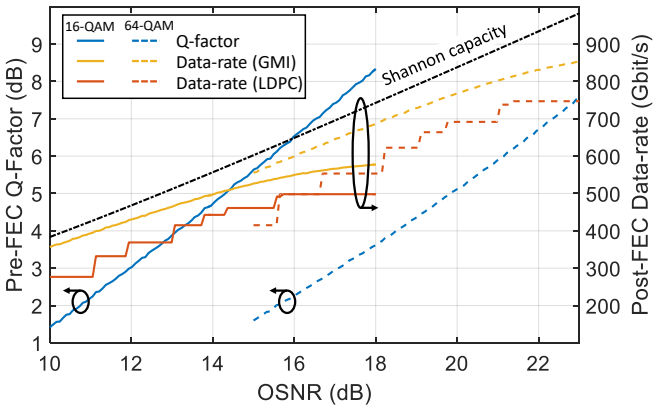

Fig. 2: AWGN simulations of a three-mode spatial super channel, based on 16- and 64-QAM. Left axis: Dashed (64-QAM) and solid (16-QAM) blue graphs show pre-FEC Q-factor. Right axis: Yellow graphs show the corresponding data rates, based on GMI estimations, red graphs show data-rates after the implemented LDPC coding scheme and Shannon capacity as a reference.

code and every column to a codeword of the inner code. On the transmitter side, data is entered row-wise and read out column-wise, while the reverse operations take place in the receiver. Although such an interleaving scheme is convenient in theory, it is in practice costly in terms of memory and latency, both given by the product of the codeword lengths. Hence, for a practical implementation, it may be beneficial to use a single FEC code that can guarantee error free transmission, instead of combining two coding stages.

Figure 2 shows AWGN simulations of the coding emulation. The graphs represent three-mode spatial super channels (SSCs) based on 24.5 GBaud PDM-16-QAM (solid lines) and 64-QAM (dashed lines). The blue lines show the pre-FEC Q-factor on the left axis, while the yellow lines represent the throughput, estimated from the GMI and the red lines show the achieved throughput with the implemented LDPC coding scheme on the right axis. A gap of up to 3 dB additional OSNR requirement, can be observed between the GMI-based throughput and the LDPC-code implementation, mainly due to the limited code-rate granularity of the DVB-2S standard. Shannon capacity is shown as reference, considering the sum of six independent 24.5 GBaud AWGN channels that compose the three-mode SSC.

IV. Experimental Setup

The experimental setup for the investigation of high data-rate transmission systems is shown in Figure 3. A comb source generated more than 400 carrier lines in a 25 GHz spacing across the C + L bands [23], [3]. The output of the comb was split into a test and a dummy channel part. The test-band was selected by a tunable filter that selected 3 or 5 carrier lines. The test band was then split into odd and even channels that were independently modulated by two dual-polarization IQ-modulators (DP-IQ). The two modulators were driven by four arbitrary waveform generators (AWGs) operating at 49 GS/s, generating 24.5 GBaud root raised cosine shaped dual polarization (DP) 16- or 64-quadrature amplitude modulated (QAM) signals with a roll-off factor of 0.01. Odd and even channels were then optically de-correlated and the C and L bands were amplified in independent amplifiers.

The dummy channel band was modulated in a separate DP-IQ modulator with 24.5 Gbaud root raised cosine shaped DP 16- or 64-QAM signals, generated by four electrically de-correlated signals generated in a single 49 GS/s AWG. The output spectrum of the dummy channels was flattened in independent C and L band optical processors (OPs), that were also used to carve a notch into the dummy channels to accommodate the test-band. Test and dummy channels were then combined and amplified. For both transmission experiments, the signals were then split into three paths that were optically de-correlated by approximately 93 ns and 193 ns to emulate independent data streams on different spatial paths. 3-D waveguide inscribed mode-selective multiplexers were used as mode multiplexers and de-multiplexers. The multiplexers had an insertion loss of approximately 1.5 dB and a mode selectivity of more than 16 dB. The total launch power per mode was approximately 25 dBm.

We used two different transmission links for this experiment. The first one was a single span of FMF, composed of 26 km negative and 4 km positive DMD fiber [24]. It is schematically shown in Fig. 4 (a) and had a resulting DMD of less than 1 ns. For the recirculating loop experiment, we added an additional 25 km of negative DMD FMF, as shown in Figure 4 (b), for a total DMD of less than 100 ps. All fiber modes had a chromatic dispersion of approximately 20 ps/nm/km and loss of approximately 0.2 dB/km. In both links, the crosstalk between LP_{01} and LP_{11} modes was less than 10 dB, measured with 2 nm amplified

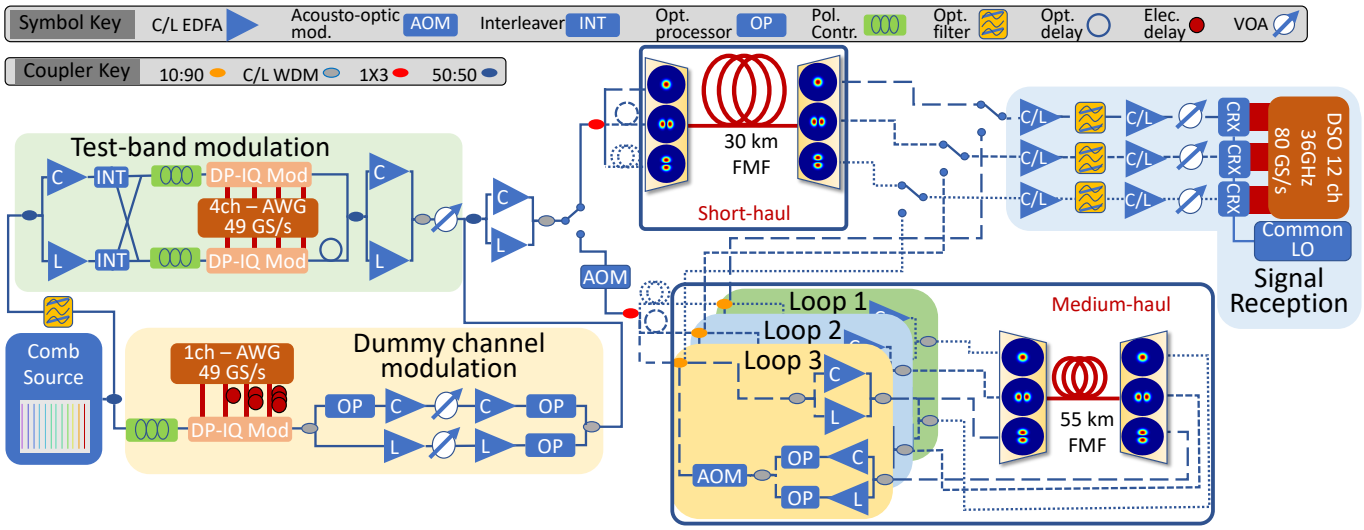

Fig. 3: Experimental Setup for the analysis of short- and medium-haul high data-rate transmission. The transmitter and receiver setups are similar for both experiments. The switches indicate the usage of different fiber links for the two described experiments. For the short-haul experiment, only a single span of FMF was used (upper center part of figure). The medium-haul transmission was achieved with a recirculating loop setup (bottom right part of figure).

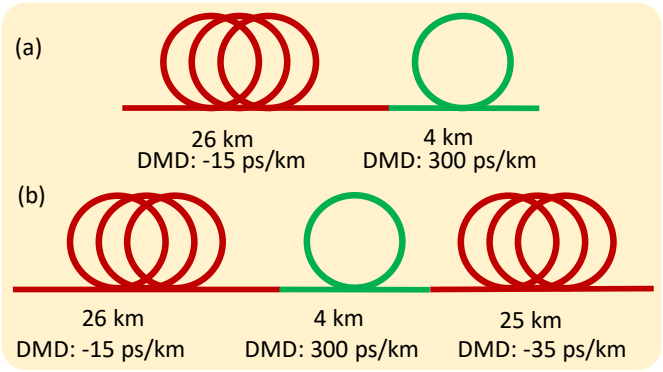

Fig. 4: Schematic description of the applied DGD management scheme.

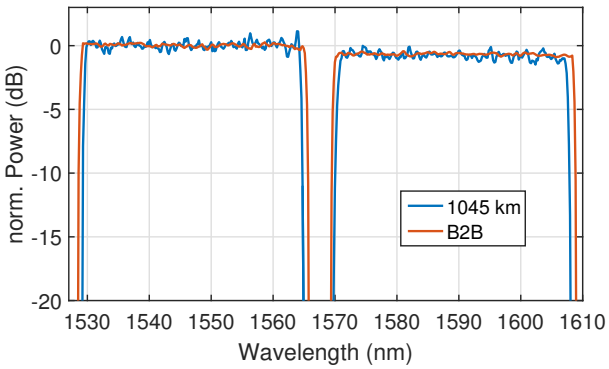

Fig. 5: OSA traces of first loop back-to-back and after 1045 km transmission.

spontaneous emission (ASE) noise.

The effective area of the fundamental mode was 124 μm^2. The effective area of the LP$_{11}$ modes can then be estimated at 165 μm^2. The fiber's large effective areas and high chromatic dispersion values indicate that the system performance should be better than with a standard single-mode fiber, when omitting MDL or intermodal nonlinear signal degradation.

For the recirculating loop setup, a single acousto-optic modulator (AOM) was used before the spatial split to gate the loop loading time. After transmission, the signals were demultiplexed and three independent single-mode stages of C + L band amplifiers and optical processors were used to amplify and flatten the spectrum of the signals that were propagated through the three fiber modes. Three AOMs were used to gate the loop timing. After a maximum of 19 recirculations, the signals from the loop-coupler were send to the receiver structure.

The receiver was composed of three independent two-stage single-mode fiber C + L band EDFAs with tunable filters to select the channel under test. The signals were mixed in three coherent receivers (CRX) with the light of a tunable external cavity laser (ECL) as local oscillator. Due to availability, the ECL in the first experiment had a nominal linewidth of 100 kHz and 10 kHz in the second experiment. The electrical signals from the three CRXs were digitized in a 12-channel oscilloscope with 36 GHz electrical bandwidth, operating at 80 GS/s. Offline digital signal processing (DSP) consisted of re-sampling to two samples per symbol, static chromatic dispersion compensation (only for long-haul transmission) and a time-domain least-mean square based multiple-input multiple-output (MIMO) equalizer with 117 taps for the short-haul link and 751 taps for the long-haul experiment. After data-aided initial convergence, the equalizer switched to a decision-directed mode. Q-factor estimation was performed after direct error counting.

V. Transmission Impairments

This section discusses transmission impairments that were observed in the recirculating loop experiment over more than 1000 km distance, first reported in [13]. Figure 5 shows traces from an optical spectrum analyzer (OSA) with a resolution of 0.2 nm of the signal in the first transmission loop, back-to-back and after 1045 km transmission. The power-spectral density in the L-band is slightly lower than in the C-band, as more channels were transmitted in the L-band compared to the C-band, while keeping the overall power equal in both bands. Furthermore, the number of transmitted channels (381) in both C- and L-band, and hence the total signal bandwidth, is slightly larger than the received signal bandwidth (348 channels) after 1045 km transmission. This is

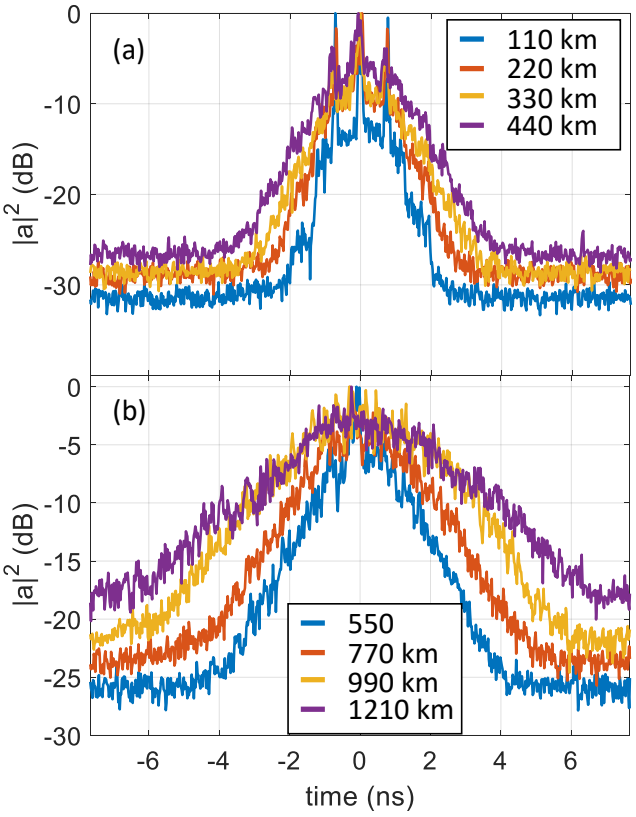

Fig. 6: Impulse responses of an SSC at 1550 nm wavelength after transmission. (a) up to 440 km, (b) up to 1210 km

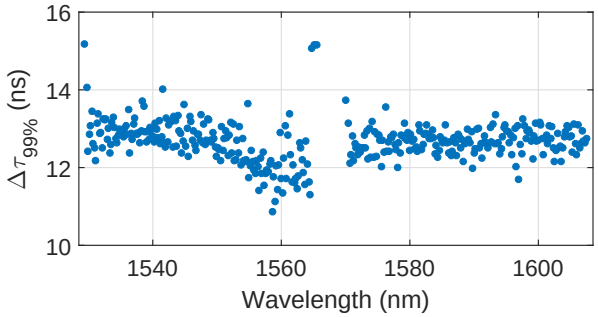

Fig. 7: Impulse response lengths for all SSC after 1045 km transmission.

mostly due to bandwidth limitations in the three loops' optical processors. We further observed a ripple in the spectrum that was dynamically changing over short times, thus prohibiting further spectral flattening. We attribute this to wavelength-dependent dynamic changes of the coupling behaviors between different spatial modes.

Figure 6 shows the impulse responses of an SSC at 1550 nm wavelength after transmission, calculated as in [13]. Figure 6 (a) shows impulse responses between 110 and 440 km. Distinct peaks can be observed within approximately 2 ns, indicating the total delay spread of a single round-trip of the loop.

The peaks can be explained by discrete mode coupling at the splices between the transmission fiber and the mode

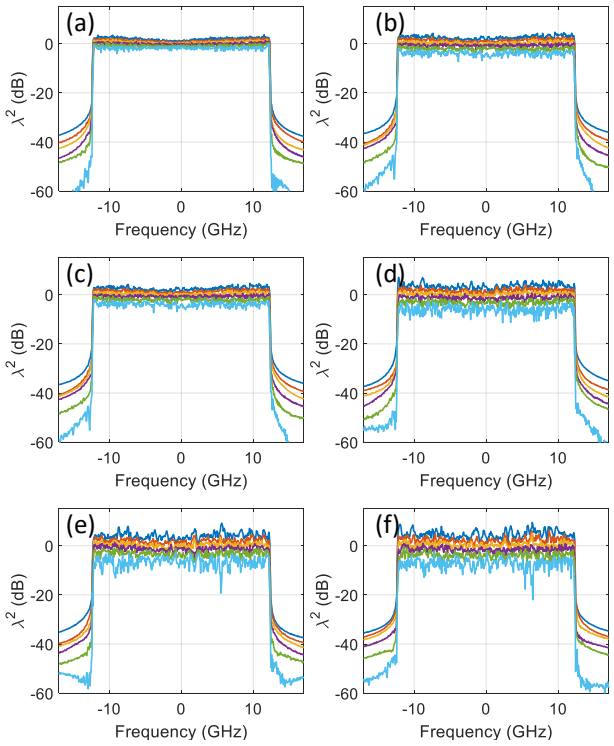

Fig. 8: Singular value decomposition after (a) 0, (b) 110, (c) 330, (d) 660, (e) 880 and (f) 1045 km transmission for an SSC at 1550 nm wavelength.

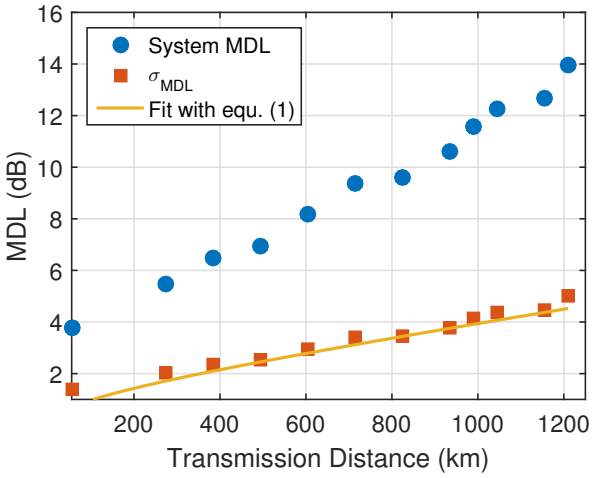

Fig. 9: System MDL, σ_{MDL}, and a fit of σ_{MDL} according to (1) as a function of transmission distance for the SSC at 1550 nm wavelength.

(de-) multiplexers, as those were not optimized for the used transmission fiber. The separation between the peaks does not significantly increase with distance, indicating that the overall loop is well aligned. However, the total delay spread increases with distances due to coupling between modes and DMD. Figure 6 (b) shows the impulse responses for longer distances up to 1210 km. The distinct peaks from Fig 6 (a) are no longer visible, while the overall impulse response further broadens. These observations indicate strong mixing between the modes occurring after transmission of more than 770 km distance.

Figure 7 shows the length of the impulse responses $(\Delta\tau_{99\%})$ for all SSCs after 1045 km transmission. $\Delta\tau_{99\%}$ is defined as the time span that covers 99% of the coefficients of the impulse response. $\Delta\tau_{99\%}$ shows almost no wavelength dependence in the L-band, while a slight wavelength-dependence can be observed in the C-band. Some edge channels in both, C and L band have increased values of $\Delta\tau_{99\%}$. We observed similar stronger impairments for the channels on the band edges for the MDL, as explained later in this section. The main cause for this is thought to be suboptimal operation of the spectral flattening algorithms, rather than physical impairments of the link. The small overall wavelength dependence of the $\Delta\tau_{99\%}$ further confirms the low DMD of the FMF across C and L bands.

Figure 8 shows the singular value decomposition of the frequency-dependent channel matrix, calculated according to [13] for the SSC at 1550 nm wavelength. When increasing the transmission distance, the six graphs increasingly deviate from each other, indicating growing mode-dependent loss. Furthermore, a strong frequency fluctuation can be observed that resembles multi-path interference and fading, observed in wireless channels.

The system MDL, defined as the ratio of the maximum to the minimum value of the frequency-averaged singular values is shown in Figure 9. The figure further shows σ_{MDL}, defined as the standard deviation of the frequency-averaged

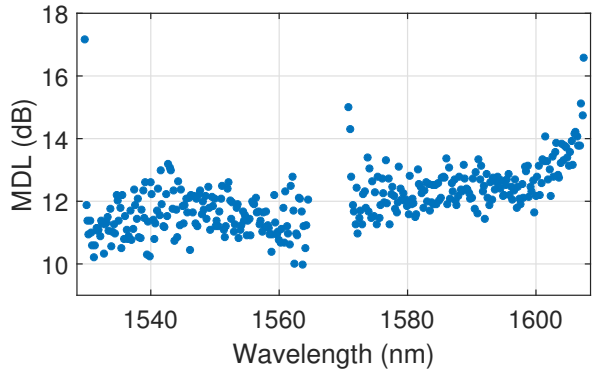

Fig. 10: System MDL for all 348 spatial super channels after 1045 km transmission distance.

singular values. Theoretical studies [25] have predicted that σ_{MDL} should increase with the square-root of the number of transmission spans as:

$$\sigma_{MDL} = \xi\sqrt{1+\frac{1}{12}\xi^2} \tag{1}$$

with $\xi = \sqrt{K}\sigma_G$, assuming strong coupling between all spatial channels. The fit in Figure 9 uses $\sigma_G = 0.7$ dB and K being the number of 55 km spans, leading to a good agreement between experimental data and the fit. We further observed an almost constant ratio between the system MDL and σ_{MDL}, which is in accordance with previous observations [14], [13].

Figure 10 shows the system MDL of all 348 spatial super channels after 1045 km transmission. The values generally range between 10 and 15 dB with a few exceptions reaching up to 17 dB. A general trend of an increased MDL with higher wavelengths can be observed. A further increase of MDL on the edges of the C and L bands. The overall wavelength dependent MDL characteristics resembles the system performance, e.g. the pre-FEC Q-factor as discussed in section VI-B.

VI. Results and Discussion

A. Short-Haul Transmission Experiment

First we investigated high data-rate, short-reach transmission over a 30 km FMF link. Unlike the first presentation of these results [9] where we assumed a fixed Q-factor threshold of 5.7 dB and corresponding FEC-overhead of 20 %, which resulted in an aggregated data-rate of 280 Tbit/s, we here applied the coding scheme as discussed in Section III. Figure 11 (a) shows the pre-FEC Q-factors of the 381 received 64-QAM based SSCs between 1528 and 1610 nm wavelength. The Q-factors vary between 5.7 and 9 dB, depending on the wavelength of the SSC. A guard-band of approximately 3 nm width between the C and L bands is imposed by limitations and tolerances of C/L band WDM couplers and EDFAs. Figure 11 (b) shows the data-rate on the left axis and the corresponding code-rate on the right axis. Blue circles are calculated based on GMI and thus show the maximum achievable data-rates under the assumptions in Section III. Red diamonds show the data-rate on the left axis and the corresponding code-rate on the right axis, calculated with the implemented LDPC coding scheme. A gap can be observed between the two methods of calculation. This gap is mainly due to the small granularity of available LDPC codes in the DVB-2S standard. The lowest overhead code-rate, including outer FEC, is approximately 0.85, while the GMI calculations indicate that a code-rate above 0.9 would be sufficient for most SSCs. Nevertheless, an aggregated data-rate of more than 283 Tbit/s is achieved with the implemented coding scheme, although the GMI calculations suggest a throughput exceeding 320 Tbit/s could be reached by using optimal coding schemes.

B. Medium-Haul Transmission Experiment

Figure 12 shows the results of the long-haul transmission experiment over 1045 km FMF. A total of 348 DP-16-QAM

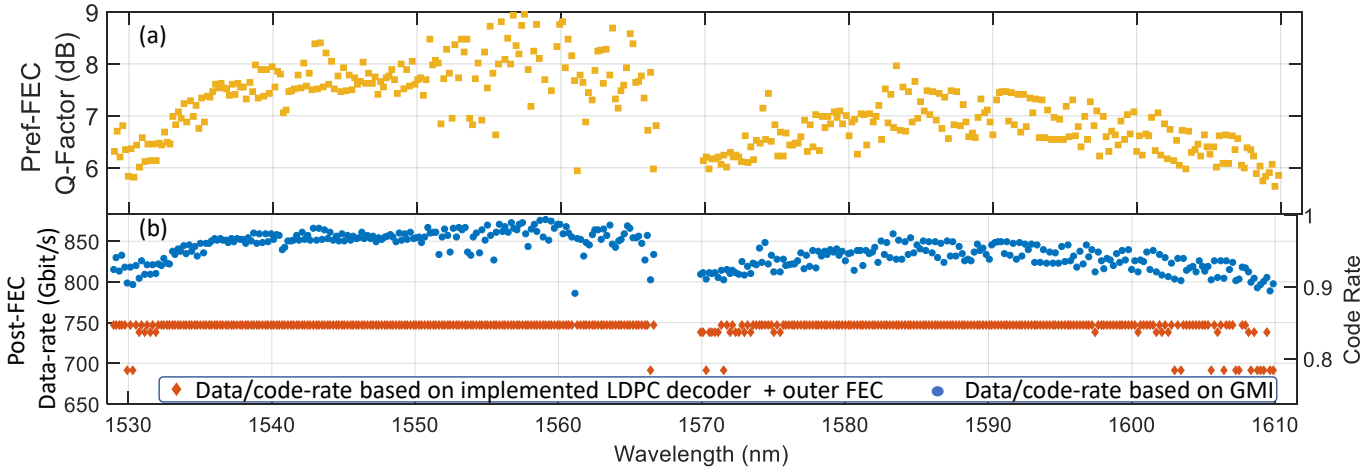

Fig. 11: (a) Q-factors of 381 64-QAM spatial super channels after 30 km transmission. (b) Blue circles show the achievable post-FEC data-rate on the left axis and the corresponding code-rates with an ideal code, calculated with the generalized mutual information. Red diamonds show the actual post-FEC data-rates and corresponding code-rates after decoding with the implemented LDPC coding scheme.

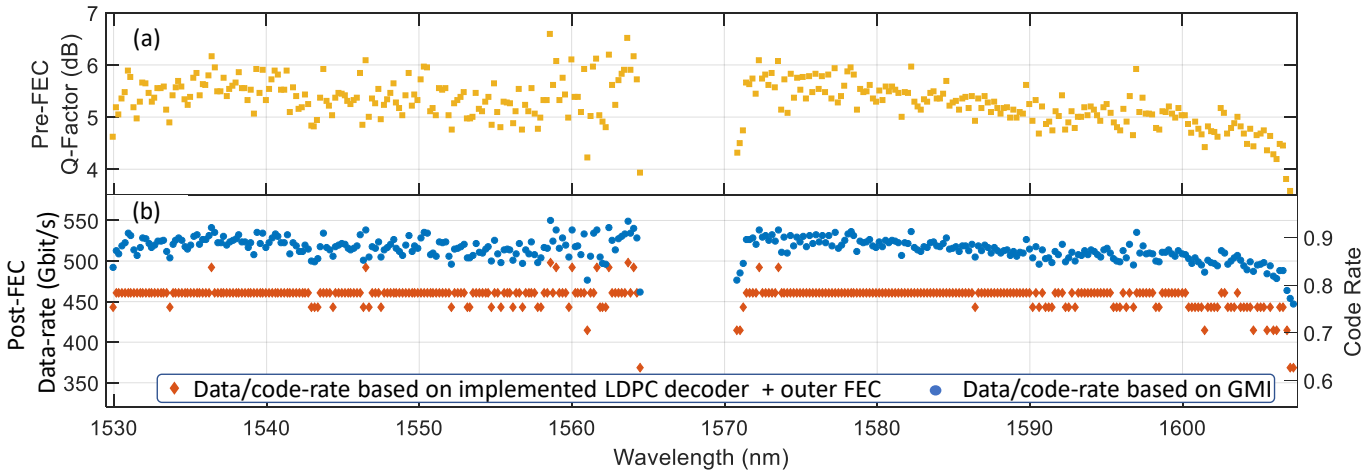

Fig. 12: (a) Q-factors of 348 16-QAM spatial super channels after 1045 km transmission. (b) Blue circles show the achievable post-FEC data-rate on the left axis and the corresponding code-rates with an ideal code, calculated with the generalized mutual information. Red diamonds show the actual post-FEC data-rates and corresponding code-rates after decoding with the implemented LDPC codes.

based SSCs were transmitted through a recirculating loop setup, described in Section IV. Figure 12 (a) shows the pre-FEC Q-factors of all SSCs. Values between 4 dB and 6.8 dB were achieved across the C + L band. The guard band between C and L band is approximately 6 nm wide, also the low C and high L band had less channels compared to the short-haul experiment reported in the previous subsection. This is mainly due to bandwidth limitations in the optical processors inside the three loop structures as well as a sub-optimal design of the applied spectral flattening algorithms.

Figure 12 (b) shows all SSCs' data-rates on the left axis and the corresponding core-rates on the right axis. Blue circles are calculated with the GMI and red diamonds are the results of the applied coding scheme. The difference between GMI based data-rates and the actual implemented FEC codes is smaller than for the short-haul experiment of the previous section. This is mostly due to the performance that is closer to the optimum for the available code-rates. The smaller difference becomes evident when calculating the aggregated throughputs: After the implemented coding scheme, a total data-rate of 159.02 Tbit/s can be reached, increasing to about 179.25 Tbit/s with the GMI based calculations for an optimum coding scheme.

VII. Conclusion

We have demonstrated high data-rate C + L band transmission in three-mode fibers based optical links for different distances. In a short-haul experiment over 30 km, we showed the transmission of more than 283 Tbit/s, with a per-mode data-rate within 10 % of the single-mode fiber record in the same wavelength bands. We then demonstrated the transmission of more than 159 Tbit/s over 1045 km three mode fiber with a record data-rate-distance-product for SDM fibers with 125μm cladding diameter of over 166 Pbit/s $\times$ km. The results demonstrate the potential of few-mode fibers to provide a capacity multiplication by the number of modes compared to current single-mode fiber technology.

References

[1] D.J. Richardson, J.M. Fini, and L.E. Nelson. Space-division multiplexing in optical fibres. Nature Photonics, 7(5):354–362, 2013.

[2] R.J. Essiambre and R.W. Tkach. Capacity trends and limits of optical communication networks. Proceedings of the IEEE, 100(5):1035–1055, 2012.

[3] B.J. Puttnam, R.S. Luís, E. Agrell, G. Rademacher, J. Sakaguchi, W. Klaus, G.M. Saridis, Y. Awaji, and N. Wada. High capacity transmission systems using homogeneous multi-core fibers. Journal of Lightwave Technology, 35(6):1157–1167, 2017.

[4] K. Kitayama and N.-P. Diamantopoulos. Few-mode optical fibers: Original motivation and recent progress. IEEE Communications Magazine, 55(8):163–169, 2017.

[5] D. Soma, Y. Wakayama, S. Beppu, S. Sumita, T. Tsuritani, T. Hayashi, T. Nagashima, M. Suzuki, H. Takahashi, K. Igarashi, I. Morita, and M. Suzuki. 10.16 peta-bit/s dense sdm/wdm transmission over low-dmd 6-mode 19-core fibre across C+L band. In European Conference on Optical Communications, page Th.PDP.A.1, Gothenburg, Sweden, 2017.

[6] S. Warm and K. Petermann. Splice loss requirements in multi-mode fiber mode-division-multiplex transmission links. Optics Express, 21(1):519–532, 2013.

[7] T. Sakamoto, T. Mori, T. Yamamoto, and T. Shigeru. Differential mode delay managed transmission line for wdm-mimo system using multi-step index fiber. Journal of Lightwave Technology, 30:2783–2787, 2012.

[8] S. Warm, G. Rademacher, and K. Petermann. Dmd management in few-mode fiber mdm transmission systems with mode coupling. In Photonics Society Summer Topical Meeting Series, 2014 IEEE, pages 158–159, 2014.

[9] G. Rademacher, R. S. Luis, B. J. Puttnam, R. Ryf, H. Furukawa, R. Maruyama, K. Aikawa, Y. Awaji, and N. Wada. 93.34 Tbit/s/mode (280 Tbit/s) transmission in a 3-mode graded-index few-mode fiber. In Optical Fiber Communication Conference, page W4C.3, San Diego, CA, USA, 2018.

[10] G. Rademacher, R. S. Luis, B. J. Puttnam, T.A. Eriksson., E. Agrell, H. Furukawa, R. Maruyama, K. Aikawa, Y. Awaji, and N. Wada. 159 Tbit/s C + L band transmission over 1045 km 3-mode graded-index few-mode fiber. In Optical Fiber Communication Conference, pages Th4C–4, San Diego, CA, USA, 2018. Optical Society of America.

[11] A. Sano, T. Kobayashi, S. Yamanaka, A. Matsuura, H. Kawakami, Y. Miyamoto, K. Ishihara, and H. Masuda. 102.3-Tb/s (224 x 548-gb/s) C-and extended L-band all-raman transmission over 240 km using PDM-64QAM single carrier FDM with digital pilot tone. In Optical Fiber Communication Conference, pages PDP5C–3, Los Angeles, CA, USA, 2012.

[12] J Cai, H G Batshon, M V Mazurczyk, O V Sinkin, D Wang, M Paskov, W Patterson, T E Subcom, and Industrial Way West. 70.4 Tb/s capacity over 7,600 km in C + L band using coded modulation with hybrid constellation shaping and nonlinearity compensation. Journal of Lightwave Technology, 36(1):114–121, 2018.

[13] G. Rademacher, R. Ryf, N.K. Fontaine, H. Chen, R.-J. Essiambre, B.J. Puttnam, R.S. Luís, Y. Awaji, N. Wada, S. Gross, N. Riesen, M. Withford, Y. Sun, and R. Lingle. Long-haul transmission over few-mode fibers with space-division multiplexing. Journal of Lightwave Technology, 36(6):1382–1388, 2018.

[14] J. van Weerdenburg, R. Ryf, J.C. Alverado-Zacarias, R.A. Alvarez-Aguirre, N. K. Fontaine, H. Chen, R. Amezcua-Correa, T. Koonen, and C. Okonkwo. 138 Tbit/s mode-and wavelength multiplexed transmission over 6-mode graded-index fiber. Journal of Lightwave Technology, 2018.

[15] D. Soma, S. Beppu, Y. Wakayama, K. Igarashi, T. Tsuritani, I. Morita, and S. Masatoshi. 257-Tbit/s weakly-coupled 10-mode C+ L-band WDM transmission. Journal of Lightwave Technology, 2018.

[16] B.J. Puttnam, R.S. Luís, Klaus W., J. Sakaguchi, J.-M. Delgado Mendinueta, Y. Awaji, N. Wada, Y. Tamura, T. Hayashi, M. Hirano, and J. Marciante. 2.15 Pb/s transmission using a 22 core homogeneous single-mode multi-core fiber and wideband optical comb. In European Conference on Optical Communication, page PDP 3.1, Valencia, Spain, 2015.

[17] A. Turukhin, H.G. Batshon, M. Mazurczyk, Y. Sun, C.R. Davidson, J.X. Chai, O.V. Sinkin, W. Patterson, G. Wolter, M.A. Bolshtyansky, et al. Demonstration of 0.52 Pb/s potential transmission capacity over 8,830 km using multicore fiber. In European Conference on Optical Communication, page Tu.1.D.3, Düsseldorf, Germany, 2016.

[18] D. Chang, F. Yu, Z. Xiao, N. Stojanovic, F.N. Hauske, Y. Cai, X. Xie, L. Li, X. Xu, and Q. Xiong. LDPC convolutional codes using layered decoding algorithm for high speed coherent optical transmission. In Optical Fiber Communication Conference, pages OW1H–4, Los Angeles, CA, USA, 2012.

[19] A. Alvarado, E. Agrell, D. Lavery, R. Maher, and P. Bayvel. Replacing the soft-decision FEC limit paradigm in the design of optical communication systems. Journal of Lightwave Technology, 33(20):4338–4352, 2015.

[20] T.A. Eriksson, T. Fehenberger, P.A. Andrekson, M. Karlsson, N. Hanik, and E. Agrell. Impact of 4D channel distribution on the achievable rates in coherent optical communication experiments. Journal of Lightwave Technology, 34(9):2256–2266, 2016.

[21] Digitalvideo Broadcasting (DVB); second generation framing structure, channel coding andmodulation systems for broadcasting, inter-active services, news gathering and other broadband satellite applications (dvb-s2), www.dvb.org/standards eur. standard etsi en 302 307 v1.2.1 (2009-08).

[22] L.M. Zhang and F.R. Kschischang. Staircase codes with 6% to 33% overhead. Journal of Lightwave Technology, 32(10):1999–2002, 2014.

[23] B. P-P Kuo, E. Myslivets, V. Ataie, E.G. Temprana, N. Alic, and S. Radic. Wideband parametric frequency comb as coherent optical carrier. Journal of Lightwave Technology, 31:3414–3419, 2013.

[24] R. Maruyama, N. Kuwaki, S. Matsuo, and M. Ohashi. Two mode optical fibers with low and flattened differential modal delay suitable for wdm-mimo combined system. Optics Express, 22(12):14311–14321, 2014.

[25] K.P. Ho and J.M. Kahn. Mode-Dependent Loss and Gain: Statistics and Effect on Mode-Division Multiplexing. Optics Express, 19(17):16612–16635, 2011.